Effects of the Azimuthal Control Jets on Structures and Entrainment of a Jet in Crossflow at Intermediate Effective Velocity Ratio 8

Pattarapol Soupramongkol and Asi Bunyajitradulya*

Department of Mechanical Engineering, Faculty of Engineering, Chulalongkorn University, Bangkok 10330, Thailand
* Corresponding Author: E-mail: asi.b@chula.ac.th, Tel: 02 218 6645, Fax: 02 218 6645

Abstract

The effects of azimuthal position of azimuthal control jets on the structures and entrainment of a jet in crossflow (JICF) at a moderate effective velocity ratio r of 8 are investigated. This research is our continuing effort in finding an effective means for manipulating and controlling entrainment of a jet in crossflow as well as evaluating the use of the azimuthal control jets in this regard. In this respect, we have reported the application of the azimuthal control jets to a JICF at low effective velocity ratio r of 4 in the past (Witayaprapakorn and Bunyajitradulya [1], Witayaprapakorn [2], and Chaikasetsin *et al.* [3]). The question still remains whether the azimuthal control jets can be as effective in manipulating, controlling, and promoting entrainment of a JICF at intermediate and higher effective velocity ratio. In the companion paper (Wangkiat *et al.* [4]), we report the use of the azimuthal control jets in the high-r regime at 12, where wall blocking of entrainment is expected to be minimal or none, while in this paper we report the use of the azimuthal control jets in the intermediate-r regime at 8, where wall blocking of entrainment may still be present. On related aspect, in order to determine the volumetric entrainment ratio more accurately, SPIV together with the jet-fluid only seeding scheme is used. This scheme does not only allow us to determine the volumetric entrainment ratio more accurately but also gives us information on the probability of finding jet-fluid mixture at a point, the jet probability structure, and the related probabilistic nature of turbulent jet. The experiment is conducted at the crossflow Reynolds number (Re_{cf}) of 3,100, and the initial jet velocity profile is fully-developed turbulent pipe flow. Two control cases are experimented; namely, a pair of azimuthal control jets is injected radially and steadily at the azimuthal positions θ = ± 15° (case I15) and ± 135° (case I135). Case I15 is the case where we found in our past work at r = 4 that it has the lowest trajectory, hence wall blocking is expected to play some role. Case I135 is the case where we found in our past work at r = 4 that it tends to have high trajectory and entrainment, hence wall blocking is less prominent. For the control cases, the azimuthal control jets to main jet mass flowrate ratio r_m is 4%. The results show that when the azimuthal control jets are applied at θ = ± 15°, the jet penetration (or wall separation) and entrainment decrease; while at θ = ± 135°, the jet penetration and entrainment increase, when compared to JICF. Moreover, I135 provides 16% higher entrainment than JICF at *x/rd* =1.5.

Keywords*:* Jet in crossflow, entrainment, flow control, azimuthal control jets, probability structure

1. Introduction

Jet in crossflow (JICF) is the flow in which a jet is injected normally into an incoming crossflow. JICF is used in applications such as mixing of fuel and air in combustors, film cooling on gas turbine blades, dispersion of pollutants from smoke stacks, and V/STOL airplanes. The governing jet characteristics that influence the effectiveness of the use of JICF in these applications are jet trajectory, entrainment, and mixing. Therefore, a technique in manipulating and controlling these governing characteristics, especially entrainment and mixing in the case of combustors, is required to improve the efficiency of these engineering equipments.

Past researches on JICF can be roughly divided into two aspects: on jet characteristics and structures and on how to manipulate and control JICF. In regard to the jet structures, Smith and Mungal [5] found that, although CVP is the main mechanism for entrainment of JICF in the far field, it does not result in entrainment enhancement over a free jet. Instead, it is the formation of the CVP in the near field that results in entrainment enhancement over that of a free jet. In regard to the formation of the CVP, Yuan *et al.* [6] proposed that the CVP is formed from hanging vortices, which in turn formed from the skewed mixing layers at the lateral edges of the jet. Yuan and Street [7] found that the jet entrainment is related to the jet trajectory by power law in the far field.

In order to manipulate and control JICF, numerous techniques have been proposed. Licinsky *et al.* [8], Zaman and Foss [9], and Bunyajitradulya and Sathapornnanon [10] investigated the use of tabs. While they are simple for passive control (fixed tabs) and possible for active control (moving/actuating tabs), there are potential complications in fabrication, operation, and maintenance of the use of tabs in hazardous environment, e.g., of hot gases. Licinsky *et al.* [8], Niederhaus *et al.* [11], Wangjiraniran and Bunyajitradulya [12], Bunyajitradulya and Sathapornnanon [10], Yinjaroen *et al.* [13], and Denev *et al.* [14], investigated the use of swirling jets. However, swirl requires relatively large amount of energy and has relatively little effect on entrainment. Eroglu and Breidenthal [15], and M'Closkey *et al*. [16] investigated the use of pulsing of the main jet. While this technique can be applied for active control but, like swirl, uses relatively large amount of energy.

Kornsri *et al*. [17] (see also Bunyajitradulya [18]) therefore proposed the use of azimuthal control jets, which use relatively less energy. They found that azimuthal control jets are effective in controlling JICF trajectory. Specifically, they found that when a pair of azimuthal control jets is deployed steadily at the azimuthal positions ($\pm\theta$) on the windward side ($\theta < 90^{\circ}$), the jet trajectory becomes lower; while on the leeward side ($\theta > 90^{\circ}$), the trajectory becomes higher, when compared to the baseline uncontrolled JICF. Witayaprapakorn and Bunyajitradulya [1] (see also Witayaprapakorn [2]) further investigated the effects of the azimuthal control jets on the jet entrainment for JICF. They found that the use of a pair of steady azimuthal control jets at $\theta = \pm 135^{\circ}$ and the control jets to main jet mass flowrate ratio (r_m) of 2% enhances entrainment by 6% over JICF at x/rd = 1.5. Chaikasetsin *et al*. [3] further investigated the effect of the azimuthal control jets to main jet mass flowrate ratio r_m, they found that at $\theta = \pm 135^{\circ}$ the increase in r_m from 2% to 4% drastically enhances entrainment, upto about 60% higher than JICF at x/rd = 1.5. Note that these past works only investigated the use of azimuthal control jets in controlling jet trajectory and entrainment for JICF with relatively low r of 4.

In regard to the effect of the effective velocity ratio r on the baseline JICF, Smith and Mungal [5] have reported that JICF can be divided into different flow regimes. Specifically, at r of 5 or lower, they reported the effects of the wall on the flow structure and entrainment while at r of 10 or higher the flow is relatively little affected by the wall. Denev *et al*. [14] and Kornsri *et al*. [17] also suggested and discussed the effect of the wall in blocking entrainment, or wall blocking. In this respect, while we have investigated the effectiveness of the use of azimuthal control jets in manipulating and controlling JICF entrainment for JICF with relatively low r of 4 already to some extent, their effectiveness when applied to JICF with intermediate r still remains unexplored. Therefore, in this work, we investigate the effectiveness of the use of azimuthal control jets in manipulating and controlling entrainment for JICF with intermediate r of 8. This is the intermediate range of r in the sense that, from past works, wall blocking may still be present to some extent.

2. Experimental Technique for the Determination of Entrainment

The time-mean accumulative volumetric entrainment ratio E is defined by

$$E = \frac{Q_j(x)}{Q_0}, \tag{1}$$

where $Q_j(x)$ is the time-mean jet-fluid mixture volume flowrate through a cross plane at location x and Q_o is the initial jet volume flowrate at the jet exit. Note that for the controlled JICF cases, Q_o is the total of the volume flowrates from both the main jet and the controll jets. The time-mean jet-fluid mixture volume flowrate $Q_j(x)$ can in turn be found from time-averaging the instantaneous jet-fluid mixture volume flowrate through the cross plane at x, $Q_j(x,t)$, over a period of time T, i.e.,

$$Q_j(x) = \frac{1}{T}\int_0^T Q_j(x,t)dt = \frac{1}{T}\int_0^T \left[\int_{A_j(x,t)} V_x(\vec{x},t)dA \right] dt, \tag{2}$$

where $V_x(\vec{x},t)$ is the instantaneous streamwise velocity field, $\vec{x}$ is the spatial position vector, and $A_j(x,t)$ is the instantaneous jet-fluid mixture cross section at location x and time t. Due to the unsteady and random nature of turbulent flow, the instantaneous jet-fluid mixture cross section $A_j(x,t)$ is also a function of time t. This results in some difficulty in determining the time-mean jet-fluid mixture volume flowrate $Q_j(x)$ and consequently the time-mean entrainment ratio E since the time-mean integral and the surface integral in Eq. (2) cannot be interchanged. If forced to interchange,

$$Q_j(x) = \int_{A_j^*(x)} V_x(\vec{x})dA, \tag{3}$$

where $V_x(\vec{x})$ is the time-mean streamwise velocity field, some less than well-defined time-mean jet-fluid mixture cross section $A_j^*(x)$ must first be chosen – with some degree of arbitrariness - from some other conditions.

Due to these difficulties and in order to give some indication of entrainment, some of the past works used indirect indicators such as decay and spread rates of some mean quantities such as mean temperature and mean passive scalar concentration, and mostly only in some limited location such as the center plane (see, e.g., Smith and Mungal [5], Wangjiranirun and Bunyajitradulya [12]). These indicators have drawbacks in that they are *indirect*: they are not a measure of volumetric entrainment ratio E directly, and/or they are *incomplete*: usually data only in limited location such as the center plane, which do not take into account the distribution of the quantity over the cross plane, are used.

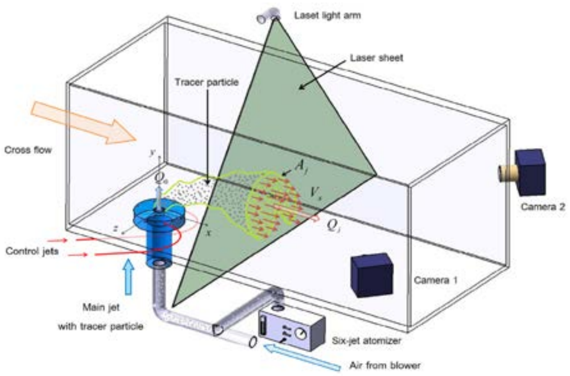

Fig. 1. Schematic diagram of the experimental setup (Chaikasetsin *et al*. [3]).

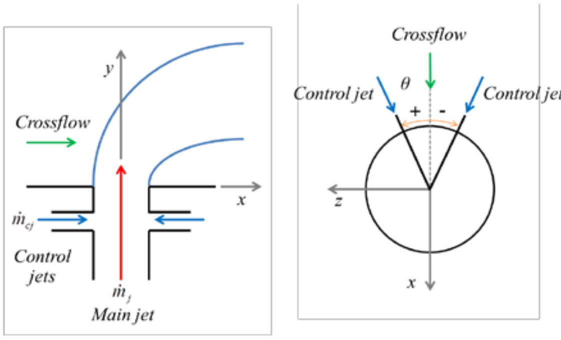

Fig. 2. Main jet and control jets configuration (Chaikasetsin *et al*. [3]).

On the other hand, in those works, notably e.g., Yuan and Street [7], that attempted to determine the time-mean accumulative volumetric entrainment ratio E more directly according to Eq. (1), due to the unavailability of the instantaneous field data, had to start off with already the *mean* field data such as mean concentration field. As a result, they are forced to set – with some degree of *arbitrariness* - threshold value for the mean scalar concentration in order to mark the jet edge in order to determine $A_j^*(x)$, and subsequently $Q_j(x)$ and E.

The problems of being indirect, incomplete, or being arbitrary to some degree, has led Wittayaprapakorn and Bunyajitradulya [1], Wittayaprapakorn [2], and Chaikasetsin *et al.* [3] to use Stereoscopic Particle Image Velocimetry (SPIV) together with the jet-fluid only – and not crossflow fluid – seeding scheme. As a result, the SPIV can measure the velocity component V_x normal to the plane of measurement (cross plane at x), and the PIV tracer particles also act as both jet-fluid markers and PIV tracers for velocity measurement. Consequently, the instantaneous jet-fluid mixture cross section $A_j(x,t)$ can be clearly and instantaneously identified and differentiated from the surrounding pure crossflow region at all times. Hence, the instantaneous jet-fluid mixture volume flowrate through the cross plane at x, $Q_j(x,t)$, can be determined at all times. Finally, the time-mean jet-fluid mixture volume flowrate $Q_j(x)$ and the time-mean accumulative volumetric entrainment ratio $E(x)$ can be determined from Eqs. (2) and (1), respectively. For further details in this regard, the reader is referred to Wittayaprapakorn and Bunyajitradulya [1], and Chaikasetsin *et al.* [3].

Finally, the effectiveness of the use of the azimuthal control jets in controlling JICF entrainment is defined by

$$\eta = \frac{E_{cJICF}}{E_{JICF}} \qquad (4)$$

where E_{cJICF} and E_{JICF} are the entrainment ratios of the controlled JICF and the baseline uncontrolled JICF, respectively.

3. Experimental Setup

3.1. Experimental apparatus

Figure 1 shows the schematic diagram of the experimental setup as well as the coordinate system used in the present work, and Fig. 2 shows the main jet and control jets assembly. The experiment is conducted in the same wind tunnel for crossflow generation as that in Wittayaprapakorn and Bunyajitradulya [1], and Chaikasetsin *et al.* [3]; the details for this part can be found in these works. To accommodate for the higher effective velocity ratios, however, the main and control jets assembly is replaced. For the present experiment, the main jet has inner diameter (d) of 12.57 mm; all control jets have inner diameter of 0.5 mm, spaced uniformly and circumferentially at 15 degrees apart, and all located 3 mm below the main jet exit plane.

3.2. Stereoscopic particle image velocimetry

To measure the three components of the velocity field (V_x, V_y, V_z) in the cross planes, a TSI™'s Stereoscopic Particle Image Velocimetry (SPIV) system is used. The SPIV laser is double cavity Nd-YAG laser (New Wave Research, Solo 200XT) with 200 mJ at 532 nm wavelength. The laser sheet is delivered to the test section by a laser light arm (model 610015) and through a laser sheet optics (model 610021-SIL, -25mm cylindrical and +500 mm spherical lenses). Two identical CCD cameras (PowerView Plus11MP, model 630062) are used to capture the PIV tracer particle images: pixel format 4008 x 2672 pixel^2, pixel size 9 µm x 9 µm, CCD size 36.07 mm x 24.05 mm, and the dynamic range of 12-bit ADC. For the imaging lenses, Tokina macro 50 mm f/1.8D lenses are used in all cases and planes, except for all cases at x/rd = 0.5 where Nikkor 100 mm f/2.8D lenses are used instead because of the smaller field of view. The laser and cameras are synchronized by a synchronizer, and the image data are processed by TSI™ Insight4G program. The tracer particles, which are 5% by volume glycerol solution, are seeded into the pipe far upstream from the main jet

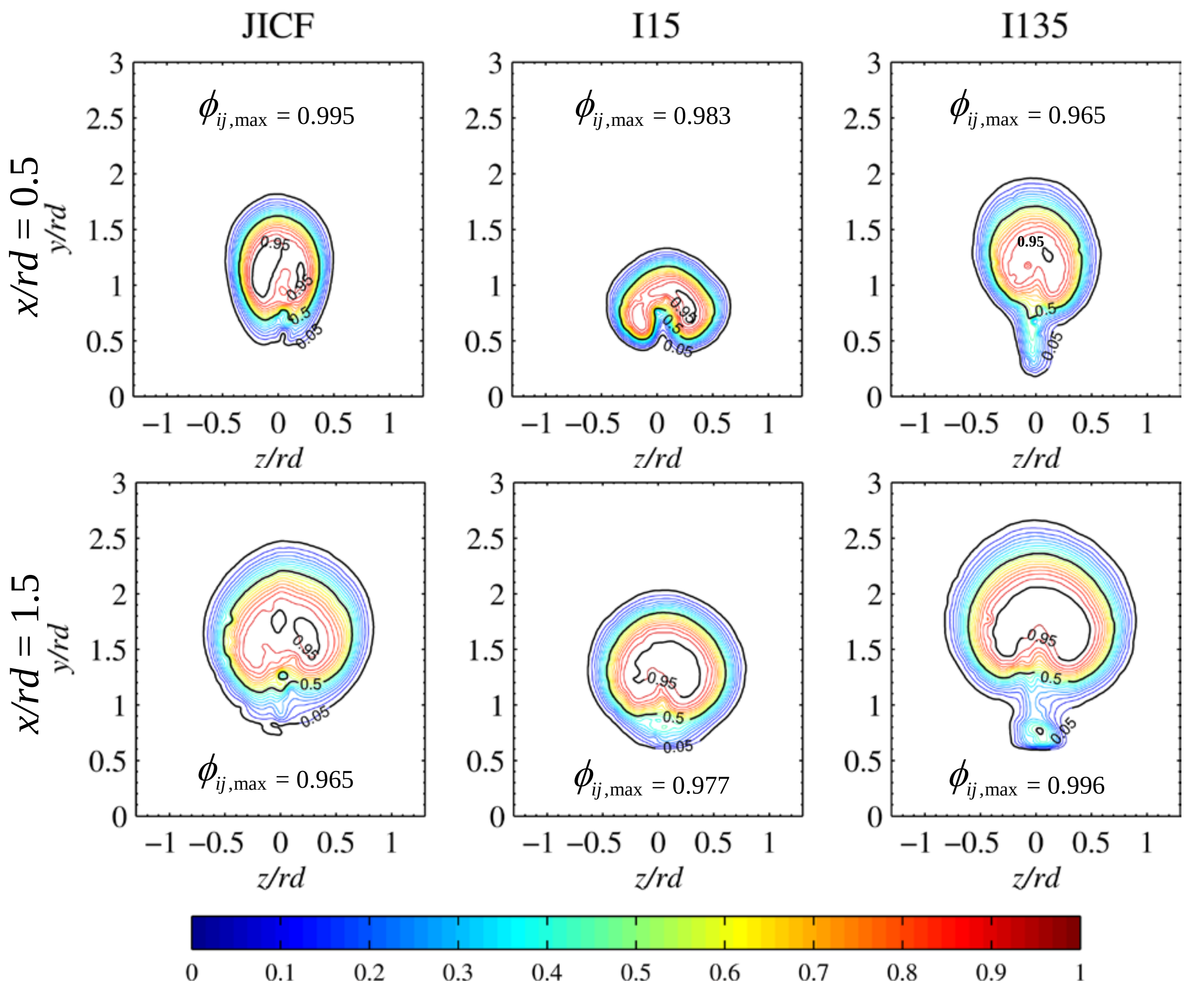

Fig. 3. Effect of the azimuthal control jets position θ on the probability of finding jet fluid at a point, ϕ_{ij}. Note that, while considered as part of the jet-fluid mixture cross section, the jet region in the range $0 < \phi_{ij} < 0.05$ is not shown in the figures. Contour line resolution is 0.05.

exit by a TSI™ six-jet atomizer to ensure uniformity of the trace particles before the main jet exit.

For the present setup, a total of 2,000 three-dimensional velocity field snapshots are used for data analysis. For the present results, the number of three-dimensional vectors in the time-mean fields are in the range of at least 6,000 to 12,000 vectors, depending on the plane, and the spatial resolutions for the vectors are 1.28 mm × 1.28 mm at x/rd = 0.5 to 1.96 mm × 1.96 mm at x/rd = 1.5.

3.3. Experimental scope and condition

The experiment is conducted at the effective velocity ratio (r) of 8.0 ± 0.3, where r is defined by

$$r = \sqrt{\rho_j u_j^{\,2} \Big/ \rho_{cf} u_{cf}^{\,2}} \tag{5}$$

where ρ is density, u is velocity, and subscripts j and cf are for main jet and crossflow, respectively. Note that for u_j, the area-averaged velocity of the main jet is used for the evaluation of r. The crossflow Reynolds Number ($\mathrm{Re}_{cf} = u_{cf} d / \nu_{cf}$) is 3,100; the jet Reynolds number ($\mathrm{Re}_j = u_j d / \nu_j$) is 24,800; and the jet initial velocity profile is fully-developed turbulent pipe flow. For the controlled JICF cases, a pair of azimuthal control jets is injected radially and steadily at the azimuthal positions, θ = ±15° (case I15) and ±135° (case I135) at the azimuthal control jets to main jet mass flowrate ratio (r_m) of 4%, where r_m is defined by

$$r_m = \dot{m}_{cj} / \dot{m}_j \,, \tag{6}$$

and $\dot{m}_{cj}$ is the total mass flowrate of the (two) control jets, and $\dot{m}_j$ is the mass flowrate of the main jet. Measurements are made at four cross planes located at the streamwise locations x/rd = 0.5, 0.75, 1.0, and 1.5.

4. Results

4.1. Effect of θ on the probability of finding jet fluid at a point

With the SPIV together with the jet-fluid only seeding scheme, we can determine the probability of

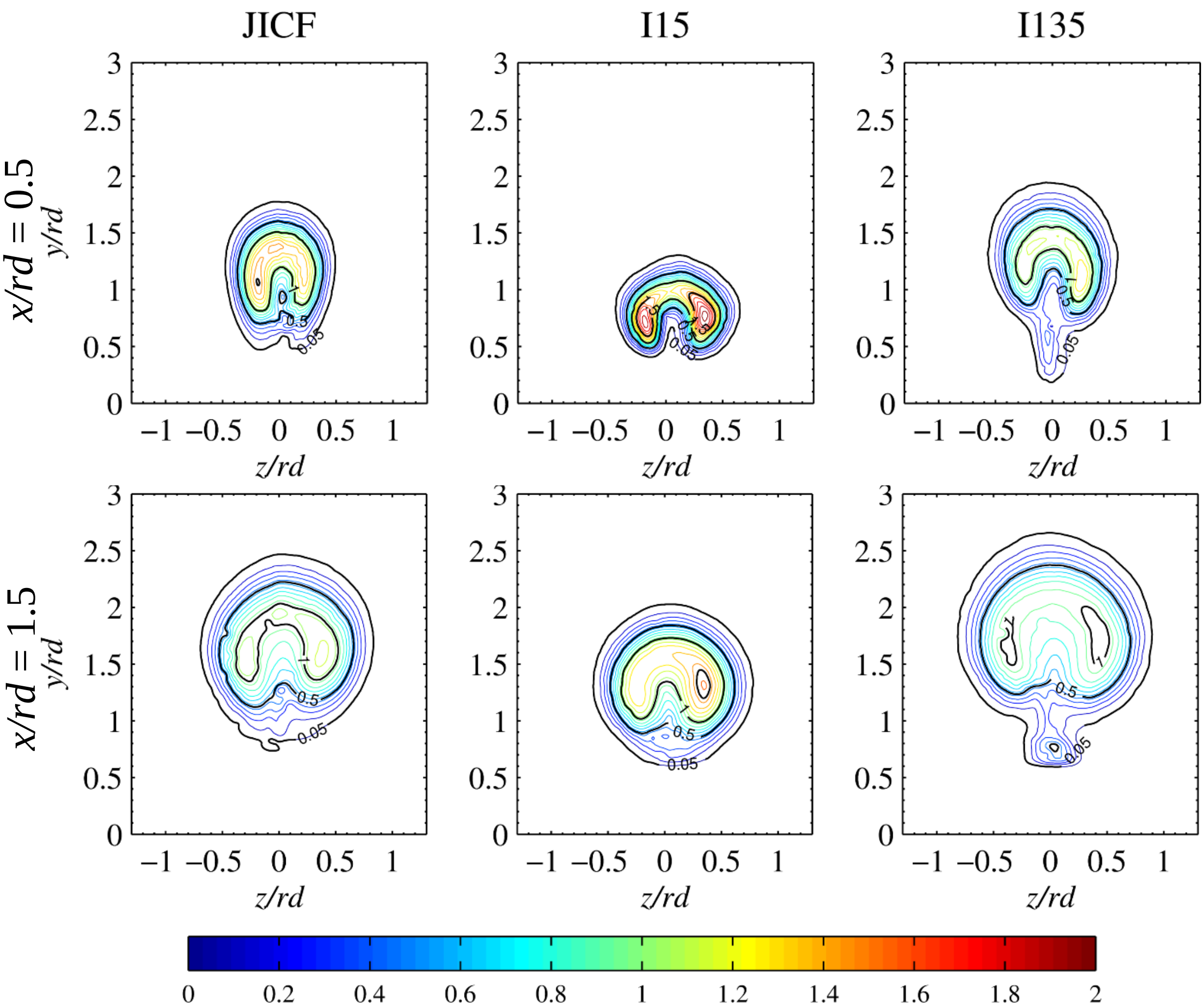

Fig. 4. Effect of the azimuthal control jets position θ on the normalized time-mean streamwise jet velocity V_x / u_{cf} . Contour line resolution is 0.1.

finding jet fluid at a spatial point ϕ_{ij} , which is defined by

$$\phi_{ij} = N_{v,ij} / N \,, \tag{7}$$

where $N_{v,ij}$ is the number of instants at which jet fluid (i.e., PIV tracer particles or the main jet fluid) is found at spatial point (i, j) , as marked by the non-zero velocity vector registered by the SPIV, and N is the total number of data-acquisition instants. In addition, the probability of finding jet fluid at a spatial point ϕ_{ij} is a complement to the probability of finding pure crossflow fluid at the point $\phi_{cf,ij}$, i.e., $\phi_{ij} + \phi_{cf,ij} = 1$.

Figure 3 shows the effects of the azimuthal control jets position θ on the probability of finding jet fluid at a point, ϕ_{ij} . Due to the jet-fluid only seeding scheme, in general ϕ_{ij} has high value near the jet center, where the probability of finding jet fluid is high; decreases and approaches zero as we approach the jet edge; and becomes zero in the pure crossflow region far away from the jet where no jet fluid can be found at all times.

The results in Fig. 3 show that overall windward injection of the control jets at I15 results in the expansion of the jet extent in the spanwise direction and the decrease in the jet penetration (or decrease in wall separation), when compared to JICF. On the contrary, leeward injection at I135 results in increase in jet penetration (or increase in wall separation), when compared to JICF. Of particular note in case I135 is the appearance of the wake-like structure at the underside of the jet, where the probability of finding jet fluid is relatively high, when compared to JICF. The figure also shows the maximum value of ϕ_{ij} for each case and plane. Overall, it is found that injection of the control jets has some slight effect on the maximum value of ϕ_{ij} , the change is no more than about 0.03, however.

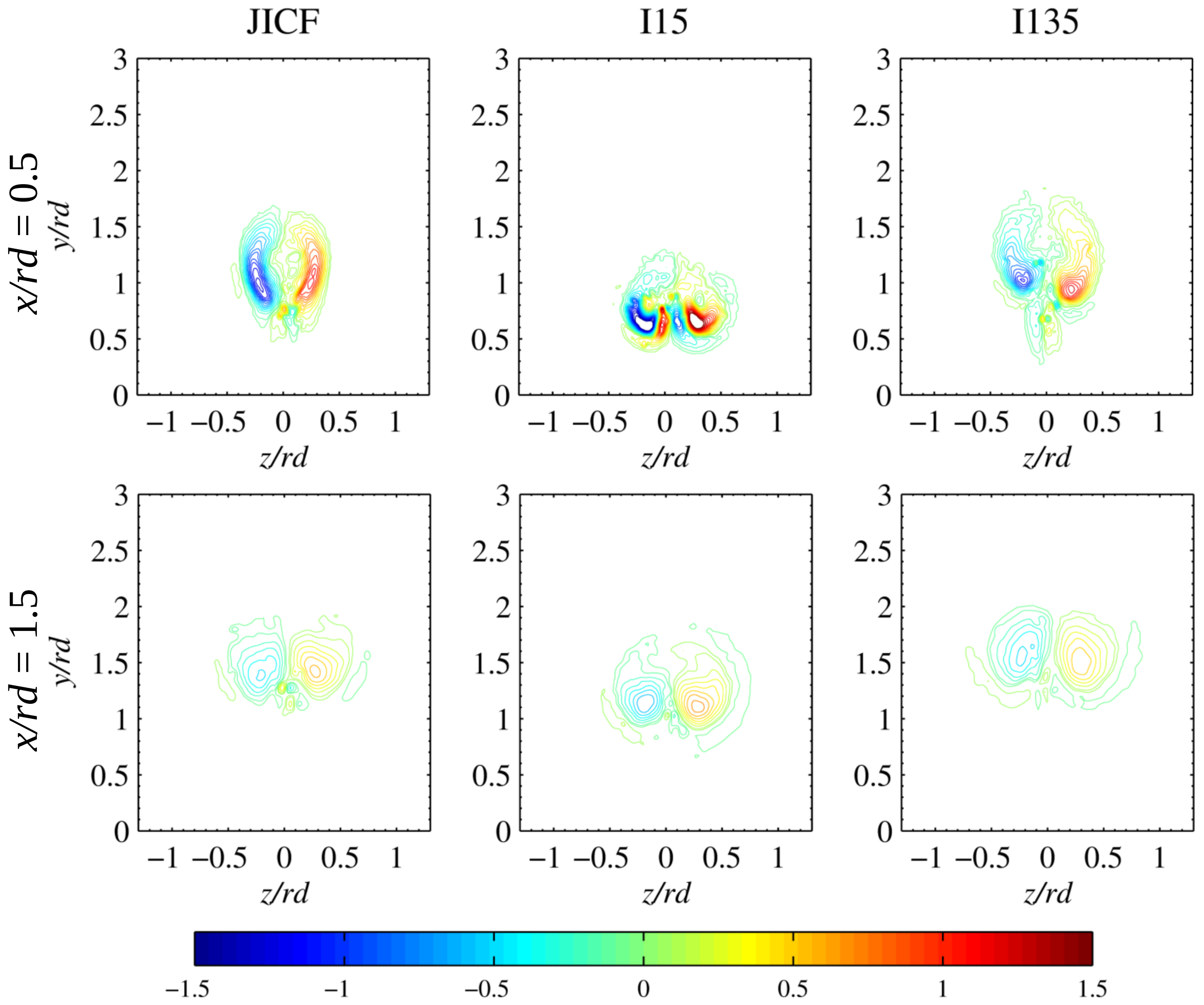

Fig. 5. Effect of the azimuthal control jets position θ on the normalized time-mean streamwise jet vorticity $\omega_x d / u_{cf}$. Contour line resolution is 0.1.

4.2. Effect of θ on the structure of the normalized time-mean streamwise jet velocity, V_x / u_{cf}

Figure 4 shows the effects of the azimuthal control jets position θ on the structure of the normalized time-mean streamwise jet velocity V_x / u_{cf} . Note that the ϕ_{ij} -structure and the V_x -structure (and any other jet field structures) must be similar in the sense that only at the point where we can find jet-fluid mixture ($\phi_{ij} > 0$) that we can have non-zero value of time-mean jet properties. The results in Fig. 4 show that windward injection at I15 results in increase in maximum streamwise jet velocity while leeward injection at I135 results in slight reduction in maximum streamwise jet velocity, when compared to JICF. In other words, windward injection at I15 causes local acceleration of the jet while leeward injection at I135 causes slight local deceleration of the jet in the streamwise direction, when compared to JICF.

4.3. Effect of θ on the structure of the normalized time-mean streamwise jet vorticity, $\omega_x d / u_{cf}$

Figure 5 shows the effect of the azimuthal control jets position θ on the structure of the normalized time-mean streamwise jet vorticity, $\omega_x d / u_{cf}$. Similar to the V_x -structure, windward injection at I15 results in increase, while leeward injection at I135 results in slight decrease, in maximum magnitude of the streamwise jet vorticity. In other words, windward injection at I15 causes local acceleration of the jet angular velocity while leeward injection at I135 causes slight local deceleration of the jet angular velocity in the streamwise direction, when compared to JICF. Note also that at upstream location, there are a few counter-rotating vortex pairs (CVP), especially case I15. As the jet develops downstream in all cases, however, there is only one dominant CVP. For all cases, as the jet develops downstream, vorticity decays in magnitude.

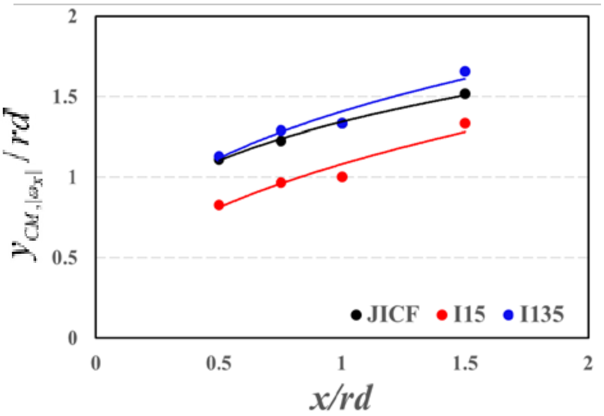

Fig. 6. Effect of the azimuthal control jets position θ on streamwise jet vorticity trajectory, $y_{CM,|\omega_x|}$.

4.4. Effect of θ on the jet trajectories

The trajectory of a jet property X (i.e., a property that is associated with jet-fluid mixture, excluding the contribution from pure crossflow fluid) is defined here as the locus of the center of mass of the absolute value, or the magnitude, of the time-mean jet property X in the transverse direction, $y_{CM,|X|}$,

$$y_{CM,|X|} = \frac{\int_{A_j} y|X|dA}{\int_{A_j} |X|dA}. \tag{8}$$

Figure 6 shows the effect of the azimuthal control jets position θ on the time-mean streamwise jet vorticity trajectory, $y_{CM,|\omega_x|}$, together with the power-law fits. In accordance with the results of Kornsri *et al.* [17], it is found that windward injection at I15 causes the jet trajectory to be lowered; while leeward injection at I135, slightly higher, than JICF. Also, the power-law fits describe the jet trajectories reasonably well.

4.5. Effect of θ on the jet entrainment and effectiveness

Figure 7(a) shows the effect of the azimuthal control jets position θ on the time-mean accumulative volumetric entrainment ratio E, together with the power-law (plus one) fits:

$$E = 1 + a(x/rd)^b. \tag{9}$$

Again, overall the results show the opposite effects of windward as opposed to leeward injection. Namely, windward injection at I15 has a tendency to suppress entrainment – especially in the near field where it also causes the jet trajectory to be lowered, while leeward injection at I135 has tendency to promote entrainment, when compared to JICF, especially in the far field.

In order to evaluate the effect of the azimuthal control jets position θ on entrainment when compared to JICF clearer, the effectiveness of the use of the

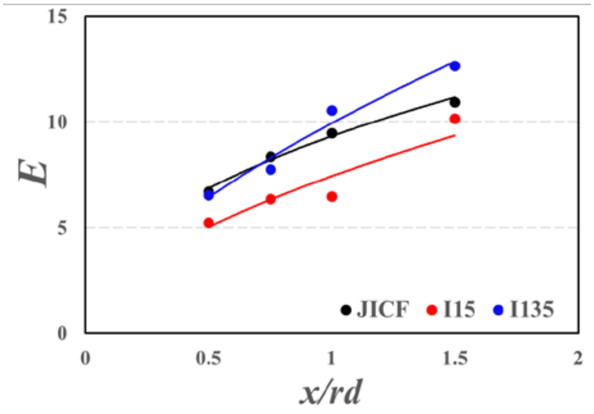

(a)

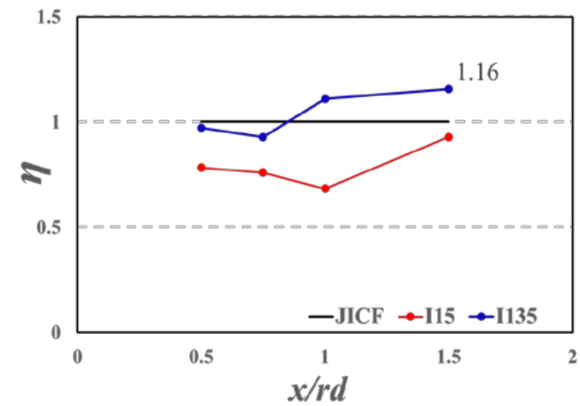

(b)

Fig. 7. Effect of the azimuthal control jets position θ on
(a) accumulative volumetric entrainment ratio E, and
(b) effectiveness η.

azimuthal control jets η is also plotted in Fig. 7(b). Overall, it can be seen that the maximum enhancement of entrainment occurs in case I135 in the far field at x/rd = 1.5, an increase by approximately 16% over JICF.

Finally, it is noted that qualitatively there seems to be correlation between trajectory and entrainment. Specifically, the higher the trajectory (the larger the wall separation), the higher the entrainment, e.g., case I135; and vice versa. This further suggests that wall blocking of entrainment (as suggested in Kornsri et al. [17] and Bunyajitradulya [18]) may still play some role in this case of JICF at intermediate r of 8. Nonetheless, this is still an unresolved issue that needs further detailed investigations.

5. Conclusion

In this work, the effects of the azimuthal control jets position θ on structure and entrainment of a jet in crossflow at the intermediate effective velocity ratio of 8 are investigated. The SPIV together with jet-fluid only seeding scheme is used in order to determine entrainment more accurately, avoiding the problems of indirect, incomplete, and/or arbitrariness, that often encountered in past works. Overall, the results show that windward injection at I15 causes 1) quite significant change in various jet structures – especially in the near field, 2) increases in both maxima of streamwise jet velocity and magnitude of streamwise jet vorticity; in other words, local acceleration of both linear and angular motion of the jet, 3) lowering of jet vorticity trajectory (or reduction in jet penetration and wall separation), and 4) reduction in entrainment, when compared with JICF. On the contrary, leeward injection at I135 causes almost the opposites; specifically, it causes 1) slight change in the jet structures – except for the appearance of the wake-like structure at the underside of the jet, 2) decreases in both maxima streamwise jet velocity and magnitude of streamwise jet vorticity; in other words, local deceleration of both linear and angular motion of the jet, 3) raising of jet vorticity trajectory (or increase in jet penetration and wall separation), and 4) enhancing in entrainment, when compared with JICF. Finally, the results also suggest that wall blocking of entrainment may still be present for JICF at this intermediate velocity ratio of 8. Nonetheless, this is still an unresolved issue that needs further detailed investigations.

6. Acknowledgements

The Thai Government Research Funds for the fiscal years 2556: Contract Nos. GRB_APS_21_56_21_04, and fiscal years 2557: Contract No. GRB_APS_23_57_21_01 are gratefully acknowledged. We would like express our appreciations for helpful suggestions and assistances to Mr. Settasit Chaikasetsin, Mr. Kittikun Wongthongsiri, Mr. Suphak Dawyok and Mr. Apichet Srimekharat; for helpful assistances and cooperations to Mr. Anand Kulpiyavaja, Mr. Apiwat Chaninwongsiri, Mr. Saran Wangkiat, Mr. Sumate Khemakanon, Mr. Apichote Kengkarnpanich, Ms. Kwanmon Sornphrom, and Ms. Minthanon Chairat.

7. References

[1] Witayaprapakorn, T. and Bunyajitradulya, A. (2013). Effects of azimuthal control jets on structure and entrainment of a jet in crossflow, paper presented in *The Twenty-Seventh Conference of the Mechanical Engineering Network of Thailand*, October 16 – 18, 2013, Chonburi, Thailand.

[2] Witayaprapakorn, T. (2013). Effects of azimuthal control jets on the entrainment of a jet in crossflow, Master Thesis, Department of Mechanical Engineering, Faculty of Engineering, Chulalongkorn University.

[3] Chaikasetsin, S., Sushewakhul, T., Panusittikorn, P. and Bunyajitradulya, A. (2014). Effects of azimuthal control jets to main jet mass flowrate ratio on the entrainment of a jet in crossflow, paper presented in *the 5th TSME International Conference on Mechanical Engineering*, December 17-19, 2014, Chiang Mai, Thailand.

[4] Wangkiat, S., Khemakanon, S., Kengkarnpanich, A., and Bunyajitradulya, A. (2015). Effects of the azimuthal positions of the azimuthal control jets on structures and entrainment of a jet in crossflow at high effective velocity ratio 12, paper presented in *the 6th TSME International Conference on Mechanical Engineering*, Cha-Am, Phetchaburi, Thailand.

[5] Smith, S.H. and Mungal, M.G. (1998). Mixing, structure and scaling of the jet in crossflow, *J. Fluid Mech*., vol. 357, pp. 83-122.

[6] Yuan, L.L., Street, R.L., and Ferziger, J.H. (1999). Large-eddy simulation of a round jet in crossflow, *J. Fluid Mech*., vol. 379, pp. 71-104.

[7] Yuan, L.L. and Street, R.L. (1998). Trajectory and entrainment of a round jet in crossflow, *Phys. Fluids*, vol. 10, no. 9, pp. 2323-2335.

[8] Liscinsky, D.S., True, B., and Holdeman, J.D. (1995). Effects of initial conditions on a single jet in crossflow, *AIAA J.*, paper no. 95-2998.

[9] Zaman, K.B.M.Q. and Foss, J.K. (1997). The effect of vortex generators on a jet in a crossflow, *Phys. Fluids*, vol. 9, pp. 106-114.

[10] Bunyajitradulya, A. and Sathapornnanon, S. (2005). Sensitivity to tab disturbance of the mean flow structure of nonswirling jet and swirling jet in crossflow, *Phys. Fluids*, 17, 045102.

[11] Niederhaus, C.E., Champagne, F.H., and Jacobs, J.W. (1997). Scalar transport in a swirling transverse jet, *AIAA J.*, vol. 35, no. 11, pp. 1697-1704.

[12] Wangjiraniran, W. and Bunyajitradulya, A. (2001). Temperature distribution in non-zero circulation swirling jet in crossflow, paper presented in *The Fifteenth Conference of The Mechanical Engineering Network of Thailand*, November 28-30, 2001, Bangkok, Thailand, vol. 1, pp. TF104-TF116.

[13] Yingjaroen, T., Pimpin, A., and Bunyajitradulya, A. (2006). Evolution of mixing regions in jet and swirling jet in crossflow: An experimental study, *Proceedings of The Twentieth Conference of The Mechanical Engineering Network of Thailand*, Nakhon Ratchasima, Thailand, 18-20 October 2006, TSF032.

[14] Denev, J.A., Fröhlich, J., and Bockhorn, H., (2009). Large eddy simulation of a swirling transverse jet into a crossflow with investigation of scalar transport, *Phys. Fluids*, 21, 015101.

[15] Eroglu, A. and Breidenthal, R.E. (2001). Structure, penetration, and mixing of pulsed jets in crossflow, *AIAA J.*, vol. 39, no. 3, pp. 417-423.

[16] M'Closkey, R.T., King, J.M., Cortelezzi, L., and Karagozian, A.R. (2002). The actively controlled jet in crossflow, *J. Fluid Mech*., vol. 452, pp. 325-335.

[17] Kornsri, P., Pimpin, A., and Bunyajitradulya, A. (2009). A scheme for the manipulation and

control of a jet in crossflow: The use of azimuthal control jets, paper presented in *The Twenty-Third Conference of the Mechanical Engineering Network of Thailand*, November 4–7, 2009, Chiang Mai, Thailand.

[18] Bunyajitradulya, A. (2011). Manipulation and control of the entrainment of a jet in crossflow, TRF RMU5080047 *Research Project Report*, Thailand Research Fund (TRF).